First measurement of the ^{34}S$(p,\gamma)^{35}$Cl reaction rate through indirect methods for presolar nova grains

S. A. Gillespie,[1,*] A. Parikh,[2,3] C. J. Barton,[1] T. Faestermann,[4,5] J. José,[2,3] R. Hertenberger,[5,6]
H.-F. Wirth,[5,6] N. de Séréville,[7] J. E. Riley,[1] and M. Williams[1,8]

[1]*Department of Physics, University of York, York, United Kingdom*
[2]*Departament de Física, Universitat Politècnica de Catalunya, Barcelona, Spain*
[3]*Institut d'Estudis Espacials de Catalunya (IEEC), E-08034 Barcelona, Spain*
[4]*Physik Department E12, Technische Universität München, D-85748 Garching, Germany*
[5]*Maier-Leibnitz-Laboratorium der Münchner Universitäten (MLL), D-85748 Garching, Germany*
[6]*Fakultät für Physik, Ludwig-Maximilians-Universität München, D-85748 Garching, Germany*
[7]*Institut de Physique Nucléaire d'Orsay, UMR8608, IN2P3-CNRS, Université Paris Sud 11, 91406 Orsay, France*
[8]*TRIUMF, Vancouver, British Columbia, Canada, V6T 2A3*

Sulphur isotopic ratio measurements may help to establish the astrophysical sites in which certain presolar grains were formed. Nova model predictions of the ^{34}S/^{32}S ratio are, however, unreliable due to the lack of an experimental ^{34}S$(p,\gamma)^{35}$Cl reaction rate. To this end, we have measured the ^{34}S$(^3$He$,d)^{35}$Cl reaction at 20 MeV using a high resolution quadrupole-dipole-dipole-dipole magnetic spectrograph. Twenty-two levels over 6.2 MeV $< E_x(^{35}$Cl$) < 7.4$ MeV were identified, ten of which were previously unobserved. Proton-transfer spectroscopic factors have been measured for the first time over the energy range relevant for novae. With this new spectroscopic information a new ^{34}S$(p,\gamma)^{35}$Cl reaction rate has been determined using a Monte Carlo method. Hydrodynamic nova model calculations have been performed using this new reaction rate. These models show that remaining uncertainties in the ^{34}S(p,γ) rate affect nucleosynthesis predictions by less than a factor of 1.4, and predict a ^{34}S/^{32}S isotopic ratio of 0.014–0.017. Since recent type II supernova models predict ^{34}S/^{32}S $= 0.026-0.053$, the ^{34}S/^{32}S isotopic ratio may be used, in conjunction with other isotopic signatures, to distinguish presolar grains from oxygen-neon nova and type II supernova origin. Our results address a key nuclear physics uncertainty on which recent considerations discounting the nova origin of several grains depend.

I. INTRODUCTION

A classical nova explosion arises from a thermonuclear runaway in a shell of hydrogen-rich material accreted onto the surface of a white dwarf star in a close binary star system (for reviews see, e.g., [1–3]). Novae are of particular interest among sites of explosive nucleosynthesis as they may be modelled using thermonuclear reaction rates that are based almost entirely upon experimental nuclear physics data. The good overall agreement of nucleosynthesis predictions with the elemental constraints provided by spectroscopy of nova ejecta suggests that isotopic signatures may also be probed. These more stringent tests of the models involve, for example, searches for cosmic γ-ray emitters such as ^{18}F, ^{22}Na, and ^{26}Al, as well as measurements of presolar grains.

Presolar grains are microscopic grains of material embedded in primitive meteorites. They are identified through isotopic ratios that differ from those in the solar system at large. Although most grains are thought to originate from supernovae and asymptotic giant branch stars, several grains have isotopic signatures (e.g., low ^{12}C/^{13}C and ^{14}N/^{15}N, high ^{30}Si/^{28}Si) that indicate a classical nova origin cannot be ruled out [4–8]. Additional signatures are evidently needed. Measurements of sulfur isotopic ratios [9–11] can provide a valuable means of discriminating between grains from novae and other stellar environments when used with other isotopic ratios indicative of nova nucleosynthesis. A recent study [12] found that the ^{33}S/^{32}S ratio may be used to distinguish between pre-solar grains of nova and supernova origin for a sufficiently precise ^{33}S$(p,\gamma)^{34}$Cl reaction rate. The predicted ^{34}S/^{32}S ratio, on the other hand, is still subject to large uncertainties as insufficient experimental information is available for the ^{34}S$(p,\gamma)^{35}$Cl reaction rate at nova temperatures; current nova models use a statistical model estimate for this rate [13]. In this work we determine, for the first time, a ^{34}S$(p,\gamma)^{35}$Cl rate based on experimental information, and we use this rate to assess the utility of the ^{34}S/^{34}S ratio as a diagnostic isotopic signature of nova presolar grains.

At temperatures encountered within nova explosions, the thermonuclear rate of the ^{34}S$(p,\gamma)^{35}$Cl reaction is dominated by resonances within $\sim$700 kev of the ^{34}S $+ p$ threshold in ^{35}Cl (S$_p(^{35}$Cl$) = 6370.82$ keV [14]). Spectroscopic studies of ^{35}Cl in this energy region have been performed only with indirect studies using the ^{32}S$(\alpha,p)^{35}$Cl reaction [15,16], through which the energies of 12 states were determined. Several direct measurements of the ^{34}S$(p,\gamma)^{35}$Cl reaction have been performed [17–19], but these were limited to states with energy $E_x(^{35}$Cl$) > 6.8$ MeV. A detailed spectroscopic study of ^{35}Cl in the 6–7 MeV excitation region is required to determine a reliable ^{34}S$(p,\gamma)^{35}$Cl reaction rate.

*stephen.gillespie.90@gmail.com

We have performed an experiment using the ^{34}S(^{3}He,d)^{35}Cl reaction to populate states in ^{35}Cl over $E_x = 6.2-7.4$ MeV. Angular distribution measurements have been used to assign J^π values and extract proton transfer spectroscopic factors for the first time in this energy region. These have been used to calculate (p,γ) resonance strengths and determine the first experimental ^{34}S(p,γ)^{35}Cl rate. Nova model calculations were performed to assess the impact of the new reaction rate on nucleosynthesis in classical novae. Finally the model predictions using our new rate are compared to pre-solar grain measurements to determine whether the ^{34}S/^{32}S isotopic ratio can be used to help identify grains of nova origin.

II. EXPERIMENT

The ^{34}S(^{3}He,d)^{35}Cl reaction was studied at the Maier-Leibnitz-Laboratorium in Garching, Germany. A 20 MeV ^{3}He^{2+} beam was accelerated by an MP Van de Graaff tandem accelerator and impinged on targets located at the entrance of a quadrupole-dipole-dipole-dipole (Q3D) magnetic spectrograph ($\Delta E/E = 2 \times 10^{-4}$) [20]. Measurements were taken with an enriched Ag$_2$^{34}S carbon backed target (50 μg/cm^2 enriched to 99.999% on 8 μg/cm^2 ^{nat}C). Contaminants were identified using measurements taken with a Zn^{nat}S target (50 μg/cm^2 on 8 μg/cm^2 ^{nat}C) and a ^{nat}C target (20 μg/cm^2). The spectrograph aperture was $d\Omega = 5.4$ msr. Reaction products were separated according to their momentum and focused on an array of focal plane detectors, consisting of two multiwire proportional counters (MWPCs) and a plastic scintillator [21]. The position of deuterons along this focal plane can be used to calculate the energies of excited states in ^{35}Cl. Deuterons were identified at the focal plane using ΔE vs E and ΔE vs ΔE information provided by the anode wires in the MWPCs and the plastic scintillator. This information was then used to produce deuteron-gated focal plane spectra. Measurements were taken at θ_{lab} = 5, 10, 15, 25, and 40 degrees, relative to the beam axis with the aim of extracting angular distributions. Spin assignments and proton transfer spectroscopic factors were extracted from these distributions and used to calculate a new ^{34}S(p,γ)^{35}Cl reaction rate.

III. DATA AND ANALYSIS

Focal plane spectra for (^{3}He,d) reactions on the Ag$_2$^{34}S, Zn^{nat}S, and ^{nat}C targets at 10° can be seen in Fig. 1. Contaminant peaks due to reactions on ^{12}C, ^{14}N, ^{16}O, ^{32}S are identified and marked with their energies given in MeV. To identify new excited states and extract peak areas for calculating angular distributions a full focal plane spectrum fit is performed using a combination of multiple Landau functions on a linear background. Contaminant states are defocused resulting in broad and ill-defined peak shapes for the states populated in reactions on ^{12}C, ^{14}N, and ^{16}O present within the Ag$_2$^{34}S target. Regions of the focal plane where contaminant states are expected are excluded from the fitting routine. The total spectrum fit at 10°, normalized to total charge collection, is shown in Fig. 2. Also seen is the contribution of individual peaks to the total fit, with isolated peaks having widths of ~10 keV FWHM.
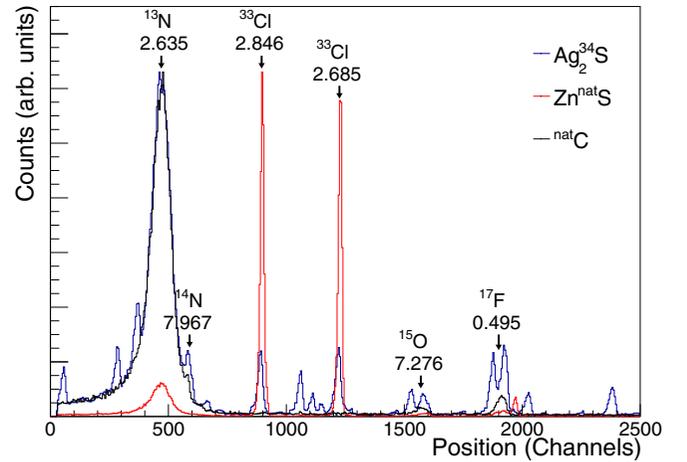

FIG. 1. 10° deuteron spectra for Ag$_2$^{34}S (blue), Zn^{nat}S (red), and ^{nat}C targets (black). The spectra have been scaled to appear on the same axis. The energies of the major contaminant peaks are marked in MeV.

The energy calibration was initially performed using the states in ^{33}Cl with energies E_x(^{33}Cl) = 2.685 and 2.846 MeV, which are known to be populated in the (^{3}He,d) reaction [22–24]. This simple two point calibration is used to identify states in ^{35}Cl known from previous ^{34}S(p,γ)^{35}Cl measurements [17,18]. These states were then used to perform an internal calibration to calculate the energy of all observed ^{35}Cl states. States which are seen at a minimum of three angles are shown in Table I, with uncertainties arising from statistics and the variance of the mean energies. An inflated excitation-energy uncertainty was assigned to the 6284 and 6329 keV levels because these energies were extracted from an extrapolation of the focal-plane calibration. Spin parity assignments are made by comparing experimental angular distributions to theoretical distorted wave Born approximation
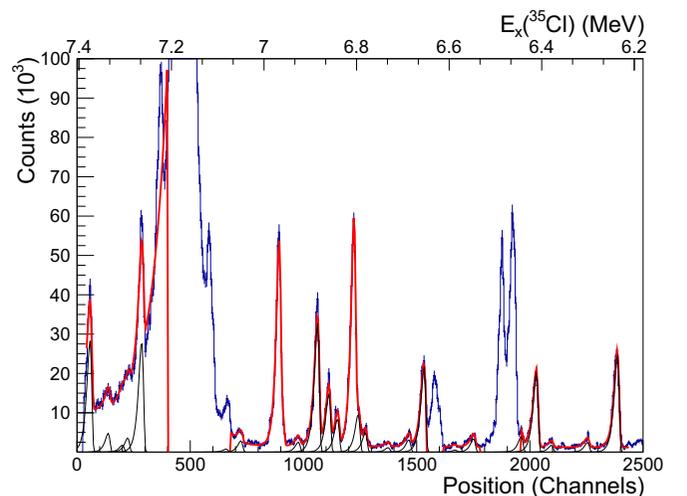

FIG. 2. Fitted deuteron spectra at 10° for the Ag$_2$^{34}S target. The total fit is seen in red with the individual peaks shown in black, see text for details.

TABLE I. Nuclear structure of ^{35}Cl for states within $6.2 < E_x < 7.4$ MeV. The first two columns give weighted averages of E_x and J^π assignments from previous ^{34}S$(p,\gamma)^{35}$Cl studies [17,18]. The next two columns give E_x and the angular momentum transfer ℓ, where the notation "/" represents two possible pure transitions and "+" indicates a mixed transition. The proton spectroscopic factors $(2J + 1)C^2S$ are given in the final column for different ℓ values with uncertainties arising from the fits of the distributions to the data.

Previous work [17,18]		Present work		
E_x (keV)	J^π	E_x (keV)	ℓ	$(2J + 1)C^2S$
–	–	6284(4)	2	0.086(2)
–	–	6329(4)	0/1	0.0030(2)/0.0044(4)
6379(3)	–	6377(2)	2/3	0.0012(6)/0.0024(8)
6427(5)	–	6427(2)	3	0.049(2)
–	–	6468(2)	1	0.034(1)
6492(2)	–	6491(2)	2	0.072(2)
–	–	6545(2)	0/1	0.004(1)/0.0028(4)
–	–	6643(2)	1	0.0144(8)
–	–	6674(2)	1/2/3	0.0020(4)/0.0048(6)/0.008(1)
–	–	6761(2)	0/1	0.0056(12)/0.0032(4)
–	–	6778(2)	1	0.0084(8)
–	–	6823(2)	1	0.006(4)
–	–	6842(2)	2/3	0.0216(6)/0.035(2)
6866.4(6)	$(1/2–5/2)^+$	6866(2)	0+2	$0.0160(2) + 0.0660(6)$
7065.9(10)	$5/2^+$	7066(2)	1/2	0.0088(8)/0.012(1)
7103.4(10)	3/2	7103(2)	1/3	0.0184(12)/0.025(2)
7178.8(10)	$1/2^+$	7178(2)	2	0.032(3)
7185.0(10)	$1/2^-$	–	–	–
7194.1(10)	$1/2^-$	7194(2)	–	–
7224.5(10)	5/2	–	–	–
–	–	7227(2)	0/1	0.065(15)/0.044(2)
7233.5(10)	$(3/2, 5/2)^+$	–	–	–
7272.8(10)	$1/2^-$	7273(2)	0/1	0.050(12)/0.030(1)
7362.1(10)	3/2	7361(2)	1	0.0040(8)
7397.0(16)	7/2	7398(2)	2/3	0.042(2)/0.0656(24)

(DWBA) calculations. These calculations were performed using the code FRESCO [25] with the global optical potentials of Liang *et al.* [26] and Daehnick *et al.* [27] for the ^{3}He and deuteron channels respectively. A fit of these calculations to the experimental data also allows for the extraction of proton transfer spectroscopic factors, C^2S [28].

The measured distributions and fits for all states seen at three or more angles can be seen in Fig. 3. The transferred orbital angular momentum, ℓ is determined from the reduced χ^2 values of the fit. For cases where multiple calculated distributions are in agreement with the data, the results are shown overlaid. In addition to pure angular momentum transfers, mixed transitions were also investigated. The extracted ℓ and $(2J + 1)C^2S$ values are given in Table I.

IV. DISCUSSION

A. ^{35}Cl spectroscopy

In total 22 states were observed over 6.2 MeV $< E_x(^{35}$Cl$) < 7.4$ MeV. Ten of these states were previously unobserved. Below 6.8 MeV this nucleus has been studied primarily in (α, p) reactions [15,16], which due to momentum matching would populate mostly high spin states. As such, the discovery of a large number of low spin states is not surprising. Above 6.8 MeV ^{35}Cl has been studied through (p,γ) reactions

[17,18] and the energies of the states found in this work are in good agreement. The energy resolution of this experiment was insufficient to resolve all known states. For example, the states at 7225 keV and 7234 keV [17,18] appear as a single peak here with an energy of 7228 keV. The triplet of states at 7179, 7185, and 7195 keV [17,18] could also not fully be resolved, with only peaks at 7179 and 7195 keV observed here. The presence of an unresolved state may explain the disagreements in spin assignments between this and the previous work. For other cases where spin-parity assignments are known there is agreement. It should be noted that it is not possible to distinguish between $J = \ell + s$ or $J = \ell - s$ coupling given the experimental uncertainties.

B. Reaction rate

The resonant component of the ^{34}S$(p,\gamma)^{35}$Cl reaction rate per particle pair is calculated using the standard formalism [29] which depends only on resonance energies E_r, resonance strengths $\omega\gamma$ and the temperature of the environment. Resonance energies were determined as $E_r = E_x(^{35}$Cl$) - Q$, where Q is the Q value of the ^{34}S(p,γ) reaction (6370.82 keV [14]). The resonance strength is defined as

$$\omega\gamma = \frac{2J_r + 1}{(2J_p + 1)(2J_T + 1)} \frac{\Gamma_\gamma \Gamma_p}{\Gamma_{\text{tot}}}, \quad (1)$$
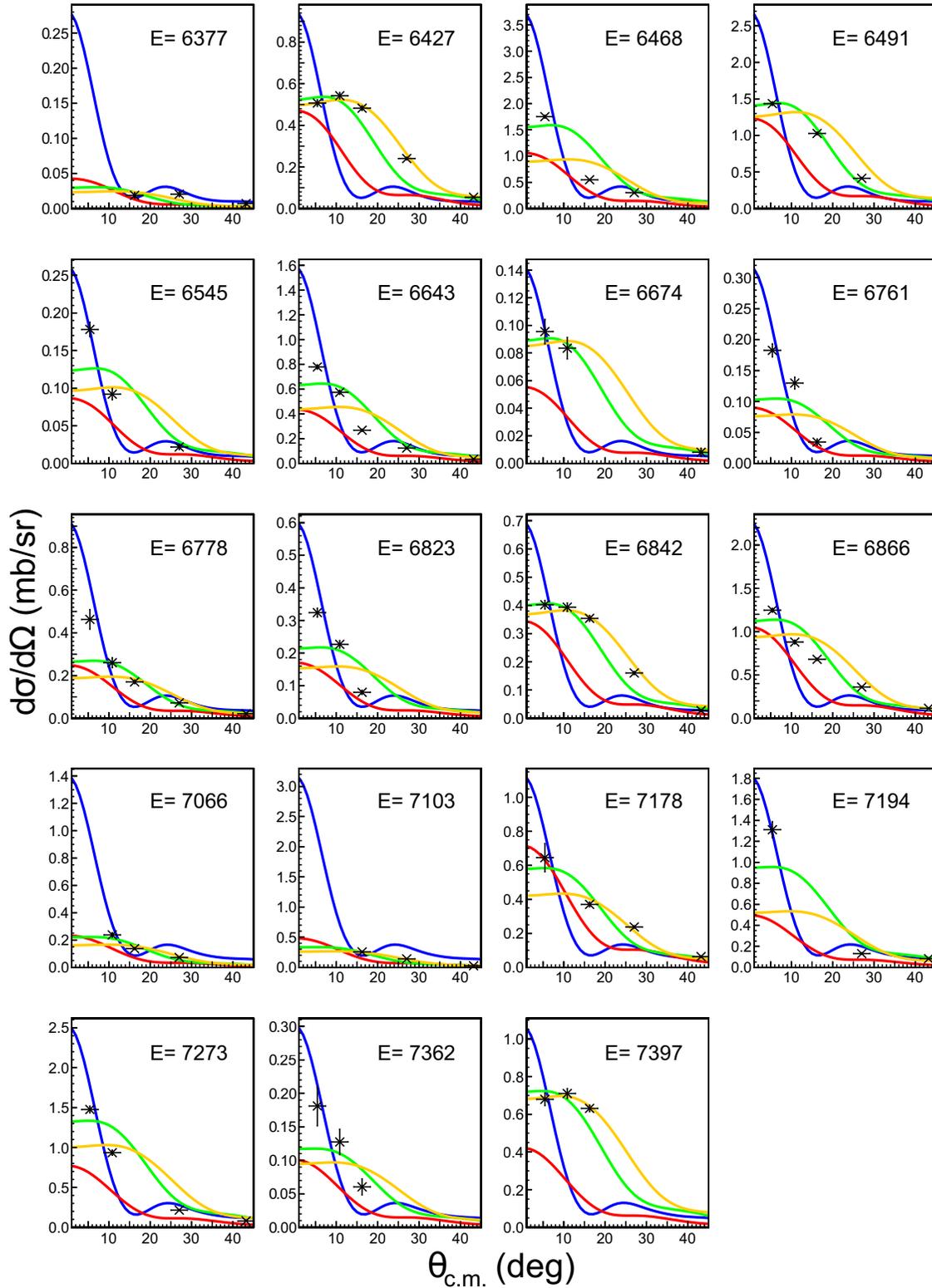
FIG. 3. Deuteron angular distributions measured with the ^{34}S(^{3}He,d)^{35}Cl reaction at 20 MeV. Graphs are fit with calculated DWBA angular distributions for angular momentum transfer $\ell = 0$ (blue), $\ell = 1$ (red), $\ell = 2$ (green), $\ell = 3$ (yellow). Extracted angular momentum transfer and spectroscopic factors from the fits are summarised in Table I. States are labeled by $E_x(^{35}$Cl) in keV. The distributions are all fit in the center of mass frame $\theta_{\text{c.m.}}$.

TABLE II. Resonance parameters for the ^{34}S$(p,\gamma)^{35}$Cl reaction. The first two columns list adopted E_x and E_r, as determined using a weighted average of present and previous works [17,18] (see Table I) and $S_p(^{35}$Cl$) = 6370.82$ keV [14]. The third column gives adopted J^π values as found through previous and present constraints [17,18]. Previously measured (p,γ) resonance strengths $\omega\gamma$ are listed in the fourth column [17,18]. The last two columns list the minimum and maximum resonance strengths used for the reaction rate calculations in this work.

Adopted E_x (keV)	E_r (keV)	J^π	Previous work [17,18,30][a] $\omega\gamma$ (eV)	Present work $\omega\gamma_{\min}$ (eV)	$\omega\gamma_{\max}$ (eV)
6427(2)	56(2)	$(5/2, 7/2)^-$	–	$6.5(2) \times 10^{-24}$	$2.2(1) \times 10^{-22}$
6468(2)	97(2)	$(1/2, 3/2)^-$	–	$4.2(5) \times 10^{-14}$	$4.7(5) \times 10^{-14}$
6491.5(8)	120.6(5)	$(3/2, 5/2)^+$	–	$3.7(1) \times 10^{-13}$	$4.1(1) \times 10^{-13}$
6545(2)	174(2)	$(1/2, 3/2)$	–	$7.4(13) \times 10^{-10}$	$4.1(1) \times 10^{-9}$
6643(2)	272(2)	$(1/2, 3/2)^-$	–	$8.5(10) \times 10^{-6}$	$8.9(10) \times 10^{-6}$
6674(2)	303(2)	$(1/2 - 7/2)$	–	$2.4(2) \times 10^{-8}$	$4.1(8) \times 10^{-6}$
6761(2)	390(2)	$(1/2, 3/2)$	–	$2.4(3) \times 10^{-4}$	$1.5(1) \times 10^{-3}$
6778(2)	407(2)	$(1/2, 3/2)^-$	–	$9.4(12) \times 10^{-4}$	$1.0(1) \times 10^{-3}$
6823(2)	452(2)	$(1/2, 3/2)^-$	–	$2.7(3) \times 10^{-3}$	$2.7(3) \times 10^{-3}$
6842(2)	471(2)	$(3/2 / 7/2)$	–	$3.3(1) \times 10^{-5}$	$7.0(3) \times 10^{-4}$
6866.4(6)	495.5(6)	$5/2^+$	$2.5(12) \times 10^{-2}$	$3.0(3) \times 10^{-2}$	$4.7(5) \times 10^{-2}$
7065.9(10)	695.1(10)	$5/2^+$	$7.0(40) \times 10^{-2}$	$2.2(1) \times 10^{-2}$	$2.2(1) \times 10^{-2}$
7103.3(10)	732.5(10)	$3/2^-$	$0.23(12)$	$6.0(3) \times 10^{-2}$	$1.30(7)$
7178.6(10)	807.8(10)	$1/2^+$	$8.1(4) \times 10^{-2}$	–	–
7185(1)	814(1)	$5/2^+$	–	–	–
7194.1(10)	823.3(10)	$1/2^-$	$0.38(19)$	–	–
7224.5(10)	853.7(10)	$5/2$	$7.6(38) \times 10^{-2}$	–	–
7233.5(10)	862.7(10)	$(3/2, 5/2)^+$	$0.52(10)$	–	–
7272.8(10)	902.0(10)	$1/2^-$	$0.59(12)$	$11(2)$	$34(3)$
7361.9(10)	991.1(10)	$3/2^-$	$0.85(17)$	$0.30(4)$	$3.0(6)$
7397.4(16)	1026.6(16)	$7/2^-$	$0.19(10)$	$0.18(1)$	$0.19(1)$

[a]It should be noted that the previous $\omega\gamma$ values were normalized to the strengths of specific reference resonances, such as the keV resonance of the ^{27}Al$(p,\gamma)^{28}$Si reaction. New $\omega\gamma$ measurements of these reference resonances, however have required these previous values to be renormalized in the evaluated data. The renormalized measurements are given here

where J_r, $J_p = 1/2$, and $J_T = 0$ are the spins of the resonance in ^{35}Cl, the proton, and the ground state of ^{34}S, respectively. The total width, proton partial widths, and γ-ray partial widths are given by Γ_{tot}, Γ_p, and Γ_γ, respectively. Proton partial widths were calculated with the expression

$$\Gamma_p = \frac{2\hbar^2}{\mu r^2} \text{C}^2\text{S} P_l \theta_{sp}^2, \qquad (2)$$

where μ is the reduced mass of the ^{34}S $+ p$ system, C^{2}S is the proton spectroscopic factor, P_l is the penetrability of the Coulomb and centripetal barriers, and θ_{sp}^2 is the single particle reduced width [29].

Resonance strengths calculated in the present work are listed in Table II. If a definite ℓ transfer could not be assigned to a state (see Table I), multiple strengths were calculated with the largest, $\omega\gamma_{\max}$, and smallest, $\omega\gamma_{\min}$, of these given in Table II. These strengths are calculated using Eq. (1) with the assumption that Γ_{tot} is dominated by the contribution from Γ_γ, so that $\omega\gamma$ depends only on Γ_p. The contribution of the α partial width has been neglected for states above $Q_\alpha = 7.0$ MeV. Considering these α partial widths would only make the relevant strengths smaller, and already, states above 7 MeV do not contribute significantly to the reaction rate at nova temperatures (see below). We have limited our treatment of uncertainties for strengths calculated in the present work to consider only those uncertainties in the ℓ transfer and in the extracted spectroscopic factors. Uncertainties in other

factors such as E_r and the adopted interaction radius will also contribute to the overall uncertainty in Γ_p.

With one exception, at keV, the previously measured $\omega\gamma$ values are in agreement with the strengths determined in the present work. A new direct measurement of the strength of the 902 keV resonance may help to clarify the origin of the discrepancy. The neglected α width of this state may also play a role in resolving this discrepancy. We do note, however, that the other calculated strengths for states above Q_α are in agreement with results from direct measurements. Nonetheless, this resonance has negligible impact on the ^{34}S(p,γ) rate over nova temperatures (see below). For the five levels between 7178 and 7234 keV, of which only three were resolved in the present experiment, we rely on strengths from previous measurements [17,18].

The reaction rate is determined through Monte Carlo methods using the STARLIB code [31] in conjunction with the information in Table II and resonance parameters for the 128 levels with 7400 keV $< E_x(^{34}$Cl$) < 9200$ keV [17–19,30]. This is the first calculation of this rate using experimental information The direct capture component was estimated with $S_{DC}(0) = 100$ keV b [13], and is negligible above $\sim$0.08 GK, at which it is less than $\sim$1% of the total rate. The upper and lower limits of the present reaction rate, along with a rate from a statistical model [32] are shown in Fig. 4. The theoretical rate clearly overestimates the ^{34}S(p,γ) rate and is found to be roughly $2-5\times$ larger than our experimental reaction rate at typical nova
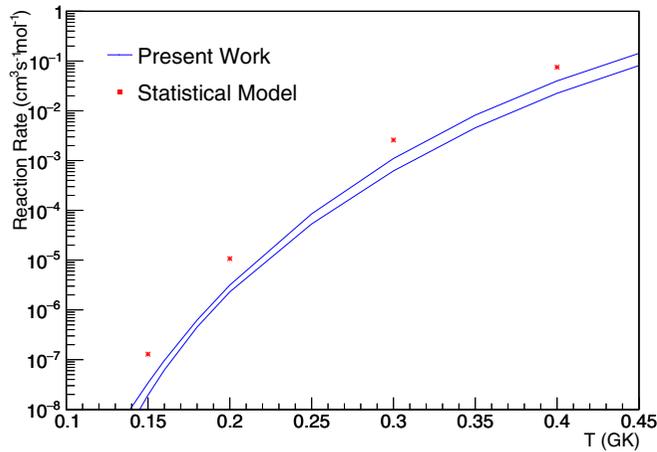
FIG. 4. Thermonuclear ^{34}S$(p,\gamma)^{35}$Cl rates over typical nova peak temperatures. Shown in blue are the low and high rates from the present work and a rate calculated using a statistical model, shown in red [13,32].

peak temperatures (e.g., 0.1–0.4 GK). The upper and lower rates differ by a less than a factor of 2 over these temperatures.

The lower limit to the reaction rate over typical nova peak temperatures is found to be dominated by a limited number of resonances with energies 272(2), 407(2), 390(2), 495(2), and 452(2) keV in order of decreasing importance. Similarly the upper limit to the rate is found to have strong contributions from the same five states with an additional contribution from the 174 keV state for $T < 0.2$ GK. The largest source of discrepancy between the high and low rates is due to the uncertainty in strengths for the 174, 390, and 495 keV resonances. Further measurements aimed at better determining the strengths of these resonances would be useful.

V. ASTROPHYSICAL IMPACT

Nova simulations were performed for the new ^{34}S$(p,\gamma)^{35}$Cl reaction rates to determine the impact of remaining rate uncertainties on nucleosynthesis predictions. The calculations were performed using a one-dimensional, spherically symmetric, implicit hydrodynamical code, known as SHIVA [33,34], which has been extensively used to model classical novae. A 1.35 M$_\odot$ oxygen-neon white dwarf was assumed, accreting matter from a companion star at the rate of 2×10^{-10} M$_\odot$yr^{-1}. The accreted matter is assumed to mix with material from the outer layers of the underlying white dwarf to a level of 50%. This level of premixing represents a simplification of the three-dimensional processes that occur at the core-envelope interface [35] and turns out to be critical for matching abundances observed in the ejecta. Nucleosynthesis results using our new low and high rates, as well as a statistical model rate (see Fig. 4) are presented in Table III. The choice of ^{34}S$(p,\gamma)^{35}$Cl reaction rate is found to affect the production of nuclei only in the S–Ca mass region, with mass fractions of other nuclei consistent within 1%. Species between $A = 34-39$ vary by less than a factor of 1.4 between the low and high rates.

Focussing on the ^{34}S/^{32}S isotopic ratio, the nova model used in this work predicts a value of 0.014–0.017 (or

TABLE III. Mean composition of nova ejecta (in mass fractions of the total ejected mass, for S - Ca isotopes) from models of nova explosions on 1.35 M$_\odot$ oxygen-neon white dwarfs. Nucleosynthesis results using the present low and high ^{34}S$(p,\gamma)^{35}$Cl rates (see Fig. 4) as well as a statistical model rate [13,32] are shown.

Nuclide	Mass fractions		
	Statistical model [13,32]	Low rate	High rate
^{32}S	5.26×10^{-2}	5.26×10^{-2}	5.26×10^{-2}
^{33}S	4.36×10^{-4}	4.36×10^{-4}	4.36×10^{-4}
^{34}S	4.71×10^{-4}	8.82×10^{-4}	7.50×10^{-4}
^{35}Cl	5.65×10^{-4}	2.69×10^{-4}	3.61×10^{-4}
^{36}Ar	7.73×10^{-5}	3.91×10^{-5}	5.18×10^{-5}
^{37}Cl	2.07×10^{-4}	1.21×10^{-4}	1.51×10^{-4}
^{38}Ar	2.96×10^{-5}	2.23×10^{-5}	2.48×10^{-5}
^{39}K	6.14×10^{-6}	5.88×10^{-6}	5.97×10^{-6}
^{40}Ca	3.06×10^{-5}	3.06×10^{-5}	3.06×10^{-5}

δ^{34}S/^{32}S $= -696 - -643$ in the notation often used for presolar grain measurements[1]) using our new reaction rates. The solar value is ^{34}S/^{32}S $= 0.047$ (δ^{34}S/^{32}S $= 0$) and recent type II supernova models predict an isotopic ratio of 0.026–0.053 (δ^{34}S/^{32}S $= -446 - 128$) [37] depending upon the initial mass of the star. This suggests that it should be possible to use the ^{34}S/^{32}S ratio to distinguish presolar grains from nova and type II supernova events.

Isotopic ratios used previously to identify nova grains have included ratios of ^{12}C/^{13}C, ^{14}N/^{15}N, ^{29}Si/^{28}Si, ^{30}Si/^{28}Si, and ^{33}S/^{32}S; nova models predict ranges of roughly 0.3–3, 0.1–10, 0.01–0.15 (δ^{29}Si/^{28}Si $= -810$–1865), 0.007–0.6 (δ^{30}Si/^{28}Si $= -804 - 15790$), and 0.0077–0.009 (δ^{33}S/^{32}S $= -53 - 107$), respectively [3,4,7,12,33]. To these we can add the δ^{34}S/^{32}S ratio predicted by the nova model adopted in the present work, $-696 - -643$. We note that nova model predictions for Si isotopes are not well constrained due to uncertainties in the ^{30}P$(p,\gamma)^{31}$S reaction rate [38,39] and that the prediction for the ^{33}S/^{32}S ratio arises from a limited study using a nova model with a single set of initial conditions [12] (as in the present study). Nonetheless the above constraints can serve as guides for diagnostic isotopic signatures of nova grains.

Grains with large, negative δ^{34}S/^{32}S values, as identified through recent measurements, are listed in Table IV. None of these grains have isotopic ratios that strictly and comprehensively satisfy predictions from nova models. Indeed for the grains KJA1-2-11-2 [9], M7-C [11], M7-D [11], and KJE-a1-5-7 [40], one of the primary indicators suggested for a nova grain, the ^{12}C/^{13}C ratio, is several orders of magnitude larger than that from nova model predictions. The grains G270_2 and Ag2_6 [41] are ostensibly more promising. Unfortunately the present nova model predicts δ^{30}Si/^{28}Si ~ 15790, which is inconsistent with all of these grains. This mismatch has been previously discussed [41] albeit with a caveat due to

---

[1]δ values are deviations from solar isotopic ratios [36] in parts per thousand, δ^{34}S/^{32}S $= [\frac{^{34}S/^{32}S_{grain}}{^{34}S/^{32}S_\odot} - 1] \times 1000$.

TABLE IV. Measured isotopic composition of selected grains with large, negative δ^{34}S/^{32}S values. Nova model predictions [3,4,7,12,33] are given in the final row for reference.

Grain ID	δ^{33}S/^{32}S	δ^{34}S/^{32}S	^{12}C/^{13}C	^{14}N/^{15}N	δ^{29}Si/^{28}Si	δ^{30}Si/^{28}Si
KJA1-2-11-2 [9]		-517 ± 88	387 ± 8	43 ± 1	1362 ± 7	1245 ± 9
M7-C [11]	-624 ± 84	-642 ± 35	152 ± 5		800 ± 15	1367 ± 21
M7-D [11]	-609 ± 61	-478 ± 142	109 ± 2		1082 ± 12	1207 ± 16
KJE-al-5-7 [40]	-944 ± 33	-941 ± 14	192 ± 1	58 ± 2	1345 ± 19	1272 ± 19
G270_2 [41]	-615 ± 385	-542 ± 175	11 ± 0.3	13 ± 0.3	-282 ± 101	-3 ± 131
Ag2_6 [41]	48 ± 334	-394 ± 106	16 ± 0.4	9 ± 0.1	-340 ± 57	263 ± 82
Nova model	$-53 - 107$	$-696 - -643$	$0.3 - 3$	$0.1 - 10$	$-810 - 1865$	$-804 - 15790$

nuclear physics uncertainties in the production of S isotopes in novae. Our results address one of these uncertainties, the ^{34}S(p,γ) rate, and, in general, confirm the results of Ref. [41]. Additional nova model calculations and grain measurements are needed to examine the possible ranges of S isotopic ratios in detail.

VI. CONCLUSIONS

We have studied the ^{34}S(^{3}He,d)^{35}Cl reaction over $E_x = 6.2-7.4$ MeV to reduce uncertainties in the ^{34}S(p,γ)^{35}Cl reaction rate over nova temperatures. Using a Q3D magnetic spectrograph ten new levels have been observed in ^{35}Cl. Proton-transfer spectroscopic factors were measured and (p,γ) resonance strengths were deduced for all levels in the relevant energy region. With this information an experimental ^{34}S(p,γ)^{35}Cl reaction rate has been calculated for the first time. Hydrodynamic nova model calculations were performed and show that remaining uncertainties in the ^{34}S(p,γ) rate

affect nova nucleosynthesis predictions by less than a factor of 1.4. The nova model used in this work predicts a ^{34}S/^{32}S isotopic ratio of 0.014–0.017. Comparing this to recent models of a type II supernova which predict ^{34}S/^{32}S $= 0.026-0.053$, it should be possible to use the ^{34}S/^{32}S isotopic ratio in conjunction with other isotopic signatures to distinguish presolar grains from oxygen-neon nova and type II supernova origin.

[1] M. F. Bode and A. Evans, *Classical Novae*, 2nd ed. (Cambridge University Press, Cambridge, 2008).

[2] J. José and M. Hernanz, J. Phys. G **34**, R431 (2007).

[3] A. Parikh, J. José, and G. Sala, AIP Adv. **4**, 041002 (2014).

[4] J. José, M. Hernanz, S. Amari, K. Lodders, and E. Zinner, Astrophys. J. **612**, 414 (2004).

[5] S. Amari, X. Gao, L. R. Nittler, E. Zinner, J. José, M. Hernanz, and R. S. Lewis, Astrophys. J. **551**, 1065 (2001).

[6] S. Amari, New Astron. Rev. **46**, 519 (2002).

[7] L. R. Nittler and P. Hoppe, Astrophys. J. Lett. **631**, L89 (2005).

[8] J. José and M. Hernanz, Meteorit. Planet. Sci. **42**, 1135 (2007).

[9] P. Hoppe, J. Leitner, E. Gröner, K. K. Marhas, B. S. Meyer, and S. Amari, Astrophys. J. **719**, 1370 (2010).

[10] F. Gyngard, F.-R. Orthous-Daunay, E. Zinner, and F. Moynier, Meteorit. Planet. Sci. Suppl. **47**, 5255 (2012).

[11] P. Hoppe, W. Fujiya, and E. Zinner, Astrophys. J. Lett. **745**, L26 (2012).

[12] A. Parikh, K. Wimmer, T. Faestermann, R. Hertenberger, J. José, H.-F. Wirth, C. Hinke, R. Krücken, D. Seiler, K. Steiger, and K. Straub, Phys. Lett. B **737**, 314 (2014).

[13] C. Iliadis, J. M. D'Auria, S. Starrfield, W. J. Thompson, and M. Wiescher, Astrophys. J. Suppl. **134**, 151 (2001).

[14] M. Wang, G. Audi, A. H. Wapstra, F. G. Kondev, M. MacCormick, X. Xu, and B. Pfeiffer, Chinese Phys. C **36**, 1603 (2012).

[15] J. D. Goss, H. Stocker, N. A. Detorie, C. P. Browne, and A. A. Rollefson, Phys. Rev. C **7**, 1871 (1973).

[16] B. W. Hooton, O. Häusser, F. Ingebretsen, and T. K. Alexander, Can. J. Phys. **48**, 1259 (1970).

[17] M. A. Meyer, I. Venter, W. F. Coetzee, and D. Reitmann, Nucl. Phys. A **264**, 13 (1976).

[18] P. Hubert, M. M. Aleonard, D. Castera, F. Leccia, and P. Mennrath, Nucl. Phys. A **195**, 485 (1972).

[19] R. J. Sparks, Nucl. Phys. A **265**, 416 (1976).

[20] M. Löffler, H. J. Scheerer, and H. Vonach, Nucl. Instrum. Methods **111**, 1 (1973).

[21] H.-F. Wirth *et al.*, Maier-Leibnitz-Laboratorium Annual Report, p. 71 (2000).

[22] R. A. Morrison, Nucl. Phys. A **140**, 97 (1970).

[23] R. L. Kozub and D. H. Youngblood, Phys. Rev. C **5**, 413 (1972).

[24] G. Inglima, R. Caracciolo, P. Cuzzocrea, E. Perillo, M. Sandoli, and G. Spadaccini, Nuovo Cimento A **26**, 211 (1975).

[25] I. J. Thompson, Comput. Phys. Rep. **7**, 167 (1988).

[26] C.-T. Liang, X.-H. Li, and C.-H. Cai, J. Phys. G **36**, 085104 (2009).

[27] W. W. Daehnick, J. D. Childs, and Z. Vrcelj, Phys. Rev. C **21**, 2253 (1980).

[28] I. J. Thompson and F. M. Nunes, *Nuclear Reactions for Astrophysics*, 1st ed. (Cambridge University Press, Cambridge, 2009).

[29] C. Iliadis, *Nuclear Physics of Stars*, 1st ed. (Wiley-VCH, New York, 2007).

[30] P. M. Endt, Nucl. Phys. A **521**, 1 (1990).

[31] A. L. Sallaska, C. Iliadis, A. E. Champange, S. Goriely, S. Starrfield, and F. X. Timmes, Astrophys. J. Suppl. **207**, 18 (2013).

[32] T. Rauscher and F.-K. Thielemann, At. Data Nucl. Data Tables **75**, 11 (2000).

[33] J. José and M. Hernanz, Astrophys. J. **494**, 680 (1998).

[34] J. José, *Stellar Explosions: Hydrodynamic and Nucleosynthesis* (CRC Press, Boca Raton, FL, 2015).

[35] J. Casanova, J. José, E. García-Berro, S. N. Shore, and A. C. Calder, Nature **478**, 490 (2011).

[36] L. Piersanti, O. Straniero, and S. Cristallo, Astron. Astrophys. **462**, 1051 (2007).

[37] A. Chieffi and M. Limongi, Astrophys. J. **764**, 21 (2013).

[38] A. Parikh, C. Wrede, and C. Fry, Eur. Phys. J. Plus **131**, 345 (2016).

[39] A. Parikh, K. Wimmer, T. Faestermann, R. Hertenberger, J. José, R. Longland, H.-F. Wirth, V. Bildstein, S. Bishop, A. A. Chen, J. A. Clark, C. M. Deibel, C. Herlitzius, R. Krücken, D. Seiler, K. Straub, and C. Wrede, Phys. Rev. C **83**, 045806 (2011).

[40] Y. Xu, E. Zinner, R. Gallino, A. Heger, M. Pignatari, and Y. Lin, Astrophys. J. **799**, 156 (2015).

[41] N. Liu, L. R. Nittler, C. M. O'D. Alexander, J. Wang, M. Pignatari, J. José, and A. Nguyen, Astrophys. J. **820**, 140 (2016).